

# Expansion of the polyQ repeat in ataxin-2 alters its Golgi localization, disrupts the Golgi complex and causes cell death

Duong P. Huynh<sup>†</sup>, Hai-Tao Yang<sup>†</sup>, Hema Vakharia, Dung Nguyen and Stefan M. Pulst\*

Rose Moss Laboratory for Parkinson and Neurodegenerative Diseases, Burns and Allen Research Institute, and Division of Neurology, Cedars-Sinai Medical Center, Departments of Medicine and Neurobiology, UCLA School of Medicine, Los Angeles, California, USA

Received February 12, 2003; Revised April 30, 2003; Accepted May 7, 2003

**Spinocerebellar ataxia type 2 (SCA2) is caused by the expansion of a polyglutamine (polyQ) repeat in ataxin-2, the SCA2 gene product. In contrast to other polyQ diseases, intranuclear inclusions are not prominent in SCA2. In animal models with expression of mutant ataxin-2 targeted to Purkinje cells, neuronal dysfunction and morphologic changes are observed without the formation of intranuclear aggregates. In this report, we investigated the mechanisms underlying SCA2 pathogenesis using cellular models. We confirmed that the SCA2 gene product, ataxin-2, was predominantly located in the Golgi apparatus. Deletion of ER-exit and trans-Golgi signals in ataxin-2 resulted in an altered subcellular distribution. Expression of full-length ataxin-2 with an expanded repeat disrupted the normal morphology of the Golgi complex and colocalization with Golgi markers was lost. Intranuclear inclusions were only seen when the polyQ repeat was expanded to 104 glutamines, and even then were only observed in a small minority of cells. Expression of ataxin-2 with expanded repeats in PC12 and COS1 cells increased cell death compared with normal ataxin-2 and elevated the levels of activated caspase-3 and TUNEL-positive cells. These results suggest a link between cell death mediated by mutant ataxin-2 and the stability of the Golgi complex. The formation of intranuclear aggregates is not necessary for *in vitro* cell death caused by expression of full-length mutant ataxin-2.**

## INTRODUCTION

Ataxin-2, the product of the spinocerebellar ataxia type 2 (SCA2) gene, is a member of a family of proteins that cause human neurodegenerative diseases, when a normal polyglutamine (polyQ) tract in the respective protein is expanded beyond a certain limit. These diseases include dentatorubral pallidoluysian atrophy (DRPLA), Huntington's disease (HD), spinobulbar muscular atrophy (SBMA), and spinocerebellar ataxias type 1, 3, 6, 7 and 17 (1–4). Although polyQ proteins are widely expressed, the primary site of pathology varies from one disorder to the other.

Normal ataxin-2 contains a polyQ repeat that most commonly contains 22 glutamines. Expansion of the polyQ repeat to 32 or longer causes a spinocerebellar ataxia type 2 (SCA2). In SCA2, mutant ataxin-2 causes neurodegeneration primarily in Purkinje neurons and selected neurons in the brain stem resulting in a progressive ataxia and death (5–8).

As in other polyQ diseases, SCA2 becomes more severe and has an earlier age of onset with increasing length of the polyQ repeat.

Studies with cellular and animal models have suggested that several factors may contribute to neurodegeneration in polyQ diseases. Individual factors may not be common to all polyQ repeat diseases. Proteins with expanded polyQ repeats often form cytoplasmic or intranuclear aggregates (4,9–15). This applies to full-length and truncated proteins, but truncation may enhance the formation of intracellular inclusions. Although aggregate formation is clearly associated with cell death, some studies have indicated that nuclear translocation rather than formation of large aggregates appears to be critical for cell death (16–18). Intranuclear inclusions of ataxin-1, 3, 7 and androgen receptor are ubiquitinated and associated with heat shock proteins indicating reduced clearance of misfolded proteins (19–24). Aggregates of mutant polyQ proteins may also trap proteins critical for cell survival (15,25). Finally,

\*To whom correspondence should be addressed at: 8700 Beverly Blvd, Davis Research Blvd, Room 2091E, Division of Neurology, Cedars-Sinai Medical Center, Los Angeles, CA 90048, USA. Tel: +1 3104235166; Fax: +1 8108212407; Email: pulst@cshs.org

<sup>†</sup>The authors wish it to be known that, in their opinion, the first two authors should be regarded as joint First Authors.

mutant polyQ proteins may stimulate the activation of caspases and may be cleaved by them leading to truncated proteins with enhanced toxicity (26–28). Although intranuclear aggregates are seen in a small number of brain stem neurons in SCA2 patients (29,30), they have not been observed in cerebellar Purkinje cells. A transgenic SCA2 animal model demonstrated that cytoplasmic localization of ataxin-2 was sufficient to cause neuronal dysfunction and altered dendritic morphology (31). We now report the effects of mutant ataxin-2 on subcellular localization and cell survival *in vitro*.

## RESULTS

While performing immunohistochemical labeling of ataxin-2 in human and mouse brain tissues, we observed that ataxin-2 often localized to cellular components resembling the Golgi apparatus (13,31,32). In this study, we utilized both biochemical and morphologic methods to determine whether ataxin-2 resided in the Golgi apparatus and to investigate the effects of the expansion of the polyQ repeat on subcellular localization and cell survival.

### Ataxin-2 co-fractionates with Golgi resident proteins in both human cerebral cortex and transiently transfected COS1 cells

To determine whether endogenous normal ataxin-2 was localized in the Golgi complex, we prepared subcellular protein fractions of frozen human cerebral cortex and transiently transfected COS1 cells using differential centrifugation. In the differential centrifugation protocol, human cerebral cortex tissues were homogenized in hypotonic buffer and centrifuged at different speeds to obtain the nuclear (P1), mitochondria/microsome (P2), Golgi complex/ER (P3), and the soluble cytosol (S3) fractions. The protein fractions were then subjected to western blotting with antibodies to the SCA2A peptide (Fig. 1A, panel a) and to the transGolgi58K protein (Fig. 1A, panel b). The SCA2A antibody recognizes a peptide immediately downstream of the polyQ repeat of ataxin-2 (13) and detected a 145 kDa band in the P3 and S3 fractions (Fig. 1A), suggesting that ataxin-2 co-fractionated with the Golgi complex and soluble protein fractions. When the same blot was detected with a monoclonal antibody to the transGolgi58K protein, an intense 58 kDa band was detected in the P3 fraction (Fig. 1A, panel b). The 58 kDa band was undetectable in the P1, P2 and S3 fractions, suggesting that the P3 fraction was greatly enriched with Golgi proteins. The 45 kDa band detected in the S3 fraction by the anti-transGolgi58K antibody is an unknown protein non-specifically detected by the anti-transGolgi58K antibody.

To investigate the effects of expansion of the polyQ repeat in ataxin-2 on subcellular localization, we transiently transfected COS1 cells with HA-tagged ataxin-2[Q22] and HA-tagged ataxin-2[Q104] expression plasmids (Fig. 1B). Subcellular fractions from transfected cells were isolated as described for the human brain tissues. One hundred micrograms of each protein fraction and whole cell extract were subjected to immunoblotting with anti-HA-conjugated peroxidase to detect HA-tagged ataxin-2, anti- $\beta$ -COP antibody to detect fractions enriched with Golgi/ER proteins in the P3 fraction (Fig. 1B,

bottom panel), and anti- $\beta$ -actin antibody (Fig. 1B) to serve as loading controls between samples containing HA-ataxin-2[Q22] and HA-ataxin-2[Q104] proteins. The anti-HA antibody detected HA-ataxin-2[Q22] and HA-ataxin-2[Q104] proteins in the whole cell extract W, S1, S2 and the Golgi/ER enriched P3 fractions. Both the HA-ataxin-2[Q22] and HA-ataxin-2[Q104] proteins were enriched in the P3 fraction, but no HA-ataxin-2 was detectable in the S3 cytosol fraction. The HA-ataxin-2 band was barely detectable in the nuclear (P1) and mitochondrial (P2) fractions. The HA-ataxin-2 was only detected in the P2 fraction with longer film exposure. The smear band shown in P1 is likely the result of overloading of cellular debris, as a shorter exposure of the same gel (Fig. 1B) reveals no specific HA-ataxin-2 band in this fraction. Despite equal transfection efficiencies and equal amounts of transfected plasmid DNAs, expression of ataxin-2[Q104] was consistently higher than that of ataxin-2[Q22]. The  $\beta$ -COP protein was enriched only in the P3 fraction consistent with the notion that the P3 fraction is enriched with Golgi-ER proteins (Fig. 1B, lower panel).

In COS1 cells, exogenous ataxin-2 was not detected in the cytoplasmic S3 fraction in contrast to human cortex shown in Fig. 1A. This discrepancy was most likely due to the fact that the human tissues were obtained several hours after death and remained frozen for months prior to protein fractionation.

### Golgi localization of ataxin-2 is altered by brefeldin A

To confirm the Golgi localization of endogenous ataxin-2, we treated COS-1 cells with brefeldin A (BFA). Brefeldin A reversibly inhibits the formation of the Golgi apparatus by blocking the transfer of proteins from the ER to the Golgi apparatus (33). Treated and untreated COS-1 cells were co-labeled with antibodies to SCA2A and the transGolgi58K protein and imaged by laser confocal microscopy. In untreated cells, ataxin-2 co-localized with the transGolgi58K protein. Besides co-localizing with the transGolgi58K protein in the peripheral Golgi network, ataxin-2 was also found in the plasma membrane, along some cytoskeletal fibers, and cytoplasmic vesicles that were not colocalized with the transGolgi58K protein (Fig. 2A, panels a–c). Treatment with BFA for 30 min caused a dispersion of both ataxin-2 and the transGolgi58K protein (Fig. 2A, panels e–g). As expected, this effect was reversible. After removal of brefeldin A and subsequent growth in culture media for an additional 1 h, ataxin-2 again co-localized with the transGolgi58K protein in the peripheral Golgi apparatus (Fig. 2A, panels i–k).

In order to investigate the effect of expansion of the polyQ repeat on the distribution of ataxin-2, we subcloned the full-length ataxin-2 cDNA containing 22, 58 or 104 CAG repeats into the pEGFP2 expression plasmids, and expressed these cDNAs in COS-1 cells. To determine whether addition of a GFP-tag altered ataxin-2 localization, we repeated the co-localization and brefeldin-A experiments. Figure 2B shows cells expressing GFP-ataxin-2[Q22] (panels a–c), and GFP-ataxin-2[Q58] (panels d–f). In untreated transfected cells (Fig. 2B, panel a), the localization of GFP-ataxin-2[Q22] was similar to that seen with endogenous ataxin-2 shown in Figure 2A. GFP-ataxin-2[Q22] was concentrated at one pole of the nucleus, and co-localized with the transGolgi58K protein

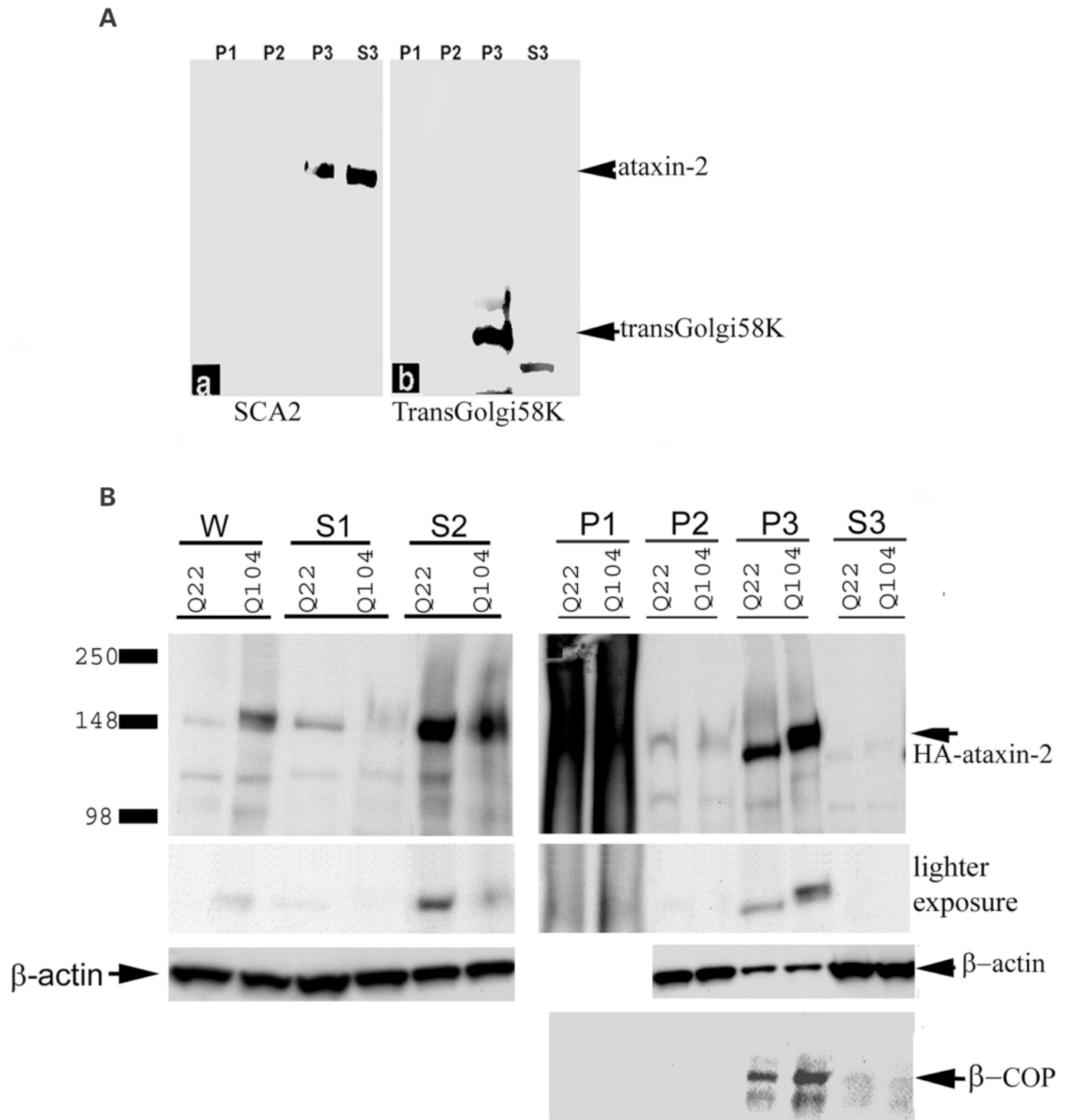


Figure 1. Analysis of ataxin-2 subcellular fractionation. (A) Western blot analysis of protein extracts obtained from subcellular differential centrifugation of human cerebral cortex. Western blots were detected with an antibody to the SCA2A peptide, and to the transGolgi58K protein. Ataxin-2 was detected in the Golgi/ER-enriched P3 and the soluble protein S3 fractions, but was undetectable in the nuclear/plasma membrane P1 and the mitochondrial P2 fractions. The Golgi resident protein, transGolgi58K, was enriched in the P3 fraction suggesting that the differential centrifugation method was effective in isolating different subcellular components. (B) Western blot analysis of protein extracts isolated by subcellular differential centrifugation from COS1 cells transiently expressing HA-ataxin-2[Q22] and HA-ataxin-2[Q104] fusion proteins. Each lane was loaded with 100  $\mu$ g of total protein. Western blots were detected with antibodies to the HA epitope at two different exposures (top two panels),  $\beta$ -actin, and  $\beta$ -COP (bottom panel). HA-tagged ataxin-2[Q22] and HA-tagged ataxin-2[Q104] fusion proteins were detected in the whole cell extract (W), S1, S2 and the final pellet P3 fractions. Both the HA-ataxin-2 and  $\beta$ -COP proteins were present in the Golgi/ER enriched P3 pellet fraction.  $\beta$ -Actin was detected in all fractions and this band was used as a control to indicate equal loading. The dark smear band in the nuclear P1 fraction is the result of overloading of the pellet extract.

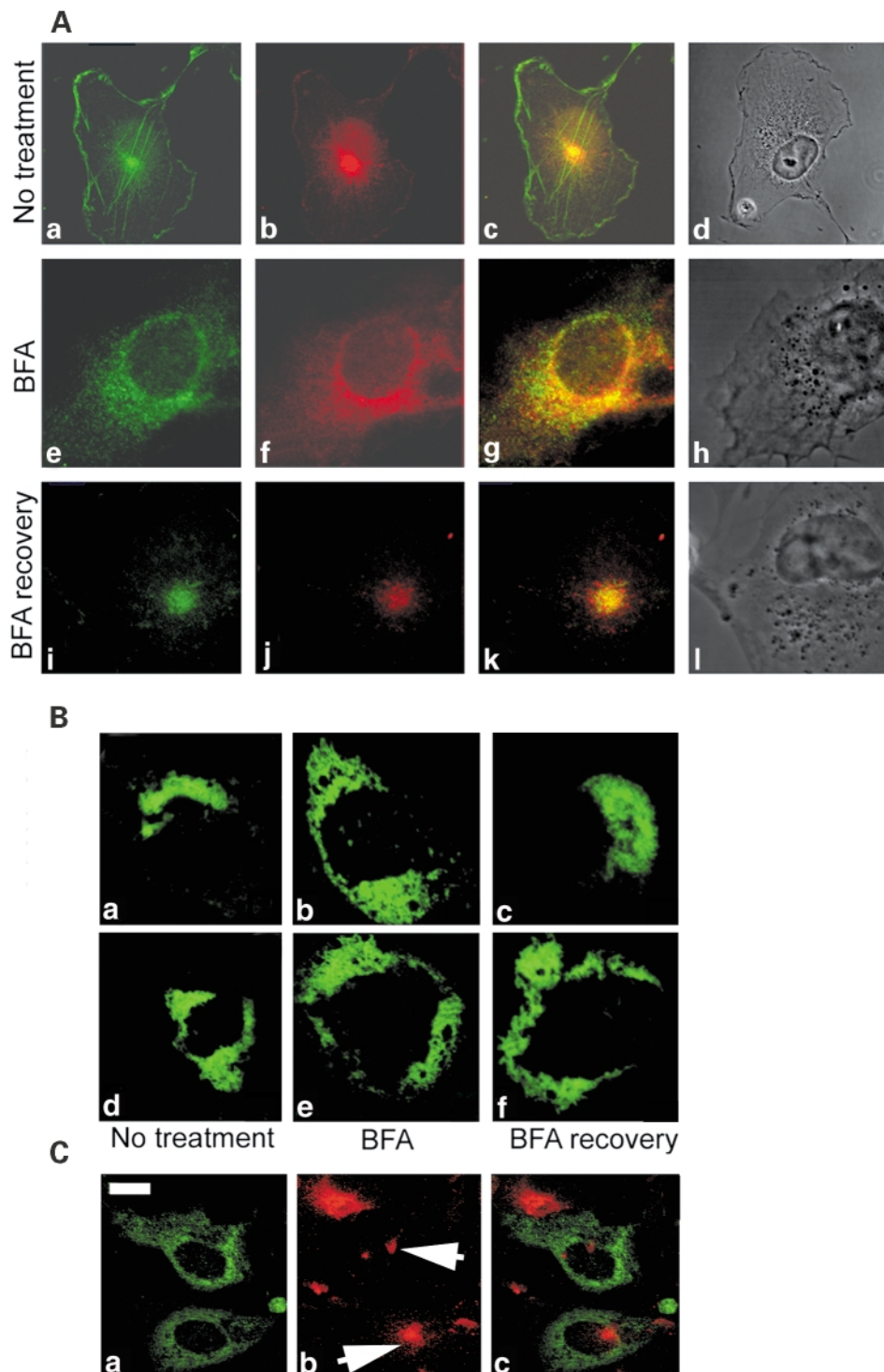


Figure 2. (A) Endogenous subcellular localization of ataxin-2 in COS1 cells. Brefeldin A (BFA) dispersed both the transGolgi58K (b, f, j) and ataxin-2 proteins (a, e, i). In untreated cells, ataxin-2 was localized with the transGolgi58K protein (panels a–c), and near the plasma membrane. BFA treatment (panels e–g) redistributed ataxin-2 and the transGolgi58K protein, and a subpopulation of the proteins was no longer colocalized. The BFA effect was reversible (panels i–k) after BFA removal for 1 h. (B) Effect of BFA treatment on COS1 cells expressing either GFP-ataxin-2[Q22] (panels a–c) or GFP-ataxin-2[Q58] (panels d–f). In untreated cells (panel a), GFP-ataxin-2[Q22] showed a typical Golgi localization in addition to some punctate staining in the cytoplasm. BFA treatment for 30 min (panel b) altered the distribution of ataxin-2. This effect was reversible after BFA removal for 1 h (panel c). BFA treatment has no effect on cells expressing GFP-tagged ataxin-2[Q58] repeats (panels d–f). (C) In-frame deletion of the putative ER/clathrin motifs altered the distribution of GFP-ataxin-2[Q22] (panel a). Transfected cells were labeled with an antibody to transGolgi58K protein (panel b), and images were overlaid (panel c). White arrows indicate transGolgi58K immunoreactivity of transfected cells. The Golgi complex was not altered by the expression of the deleted wild-type ataxin-2. Images were taken by sequential confocal laser microscopy. Scale bar, 16  $\mu$ m.

(Fig. 2B). Some GFP-ataxin-2[Q22] was also seen in small vesicles in the cytoplasm and around the plasma membrane similar to the distribution found for endogenous ataxin-2 when images were taken at a longer exposure time (data not shown). Treatment with BFA resulted in a diffuse cytoplasmic distribution of GFP-ataxin-2[Q22] (Fig. 2B, panel b) that was reversible after withdrawal of BFA (Fig. 2B, panel c). In cells expressing GFP-ataxin-2[Q58], the GFP-ataxin-2[Q58] proteins were distributed throughout the cytoplasm (Fig. 2B and 3A, panel d). Treatment with BFA produced little effect on the distribution of GFP-ataxin-2[Q58] (Fig. 2B, panel e) since expansion of the polyQ repeats redistributed the ataxin-2 protein from its localization in the Golgi complex.

**Deletion of a short domain containing both the ER exit and clathrin-mediated signals alters the distribution of the GFP-tagged ataxin-2**

Full-length ataxin-2 contains a putative ER exit motif and a putative clathrin-mediated signal (32). The ER exit signal is needed to export a particular protein from the ER, while the clathrin-mediated signal is required for clathrin-mediated cleavage from the ER, the Golgi apparatus, or the plasma membrane. We deleted both putative motifs contained in a domain of 43 amino acids; these constructs are designated ataxin-2[del43]. Cells expressing GFP-ataxin-2[Q22, del43] exhibited a distribution pattern similar to that seen with cells treated with BFA (Fig. 2C, panel a). Co-labeling with an antibody to the transGolgi58K protein showed that deletion of the putative ER-clathrin-mediated signals did not alter the structure of the Golgi complex (Fig. 2C, panels b and c). These observations suggest that these putative Golgi/ER signals are functional.

**Expansion of the PolyQ repeat disrupts the Golgi localization of ataxin-2 and causes dispersion of the Golgi apparatus**

To investigate the effect of expansion of the polyQ repeat on the subcellular localization of ataxin-2, we transiently transfected COS1 cells with GFP-ataxin-2[Q22], GFP-ataxin-2[Q58], or GFP-ataxin-2[Q104] expression plasmids. After 48 h, cells were immunofluorescently labeled with a monoclonal antibody to the transGolgi58K protein, and the labeled cells were viewed with confocal laser microscopy (Fig. 3). As shown above, GFP-ataxin-2[Q22] (Fig. 3A, panels a–c) co-localized with the transGolgi58K protein. The morphology of the Golgi apparatus appeared normal in cells expressing the GFP-ataxin-2[Q22].

However, as the length of the polyQ repeats increased, ataxin-2 was no longer localized in the Golgi apparatus, and the Golgi staining appeared to be disrupted. In cells expressing GFP-ataxin-2[Q58] (Fig. 3A, panels d–f) and GFP-ataxin-2[Q104] (Fig. 3A, panels g–i), the GFP-ataxin-2 and the transGolgi58K proteins were no longer co-localized. GFP-ataxin-2 mutants were distributed throughout the cytoplasm in a majority of transfected cells. Approximately  $67.2 \pm 2.4\%$  of the cells expressing GFP-ataxin-2[Q58] showed evidence of Golgi complex alteration. In these cells, the transGolgi58K immunolabeling was no longer concentrated in the Golgi complex, but

rather redistributed to multivesicular bodies. As the polyQ repeat expanded further, the number of cells with abnormal Golgi staining increased. In cells expressing GFP-ataxin-2[Q104],  $95 \pm 1.6\%$  of the transfected cells showed evidence of abnormal transGolgi58K immunolabeling. The transGolgi58K was found in small discrete vesicles (Fig. 3A, panel h, white arrow), whereas untransfected cells retained their normal Golgi labeling (Fig. 3A, panels i, k–l, blue arrow).

In cells expressing GFP-ataxin-2[Q104], a small fraction of the transfected cells formed intranuclear aggregates containing GFP-ataxin-2[Q104] (Fig. A, panel i, yellow arrows). The formation of intranuclear aggregates correlated with the length of the polyQ repeat and the time after transfection. There were no intranuclear aggregates in cells expressing GFP-ataxin-2[Q58] for 72 h, or in cells expressing GFP-ataxin-2[Q104] for 24 h. However, intranuclear aggregates were found in 3 of 375 cells (0.8%) expressing GFP-ataxin-2[Q104] for 48 h, and in 10 of 380 cells (2.7%) expressing GFP-ataxin-2[Q104] for 72 h.

Similar observations were made in cells transfected with GFP-ataxin-2 and labeled with an antibody to  $\gamma$ -adaptin, another peripheral Golgi protein. COS1 cells expressing GFP-ataxin-2[Q104] at 24 h were immunolabeled with the  $\gamma$ -adaptin antibody (Fig. 3A, panels j–l). Cells overexpressing GFP-ataxin-2[Q104] (Fig. 3B, panel j) were less immunoreactive with the  $\gamma$ -adaptin antibody than untransfected cells (Fig. 3A, panels k and l, blue arrow).

To investigate the possibility that the large GFP tag may influence the effect of the expanded polyQ repeat in altering the Golgi complex, we transfected COS1 cells with pcDNA-ataxin-2[Q22] (Fig. 3B, panels a–c) or pcDNA-ataxin-2[Q58] (Fig. 3B, panels d–f) that express untagged ataxin-2. These cells were colabeled with an antibody to ataxin-2 (SCA2A) and an antibody that recognizes polyQ repeats (1C2). As expected, the SCA2A antibody labeled both transfected and untransfected cells. In untransfected cells (white arrows), the SCA2A antibody strongly labeled a unipolar structure (Fig. 3B, panels a and d) that are immunoreactive for the transGolgi58K protein (Fig. 2). In transfected cells expressing ataxin-2[Q22], the SCA2A antibody labeled a similar cellular structure, although the labeling was more intense and diffuse resulting from overexpression of the exogenous ataxin-2 (Fig. 3B, panel a). In cells expressing ataxin-2[Q58], the SCA2 antibody labeled discrete aggregates around the nucleus, suggesting that expansion of the polyQ repeats recruits the formation of aggregates perinuclearly. In transfected cells, both the SCA2 and the 1C2 antibodies colocalized, although the 1C2 antibody was previously thought to stain only proteins containing long polyQ repeat. Although the 1C2 antibody labels the ataxin-2[Q22] expressing cells, it does not stain ataxin-2 in untransfected cells.

To examine whether the alteration of the Golgi complex was a result of the levels of the exogenous ataxin-2 mutant, we compared the incidence of Golgi complex disruption in cells expressing barely detectable levels of GFP-ataxin-2 mutants with those expressing 2–5-fold more ataxin-2. A total of 89 cells expressing GFP-ataxin-2[Q58] and 90 cells expressing GFP-ataxin-2[Q104] were examined. There were no differences in the incidence of Golgi alteration in cells expressing lower and higher levels of GFP-ataxin-2[Q104]. Golgi disruption was also observed in cells expressing different levels of exogenous

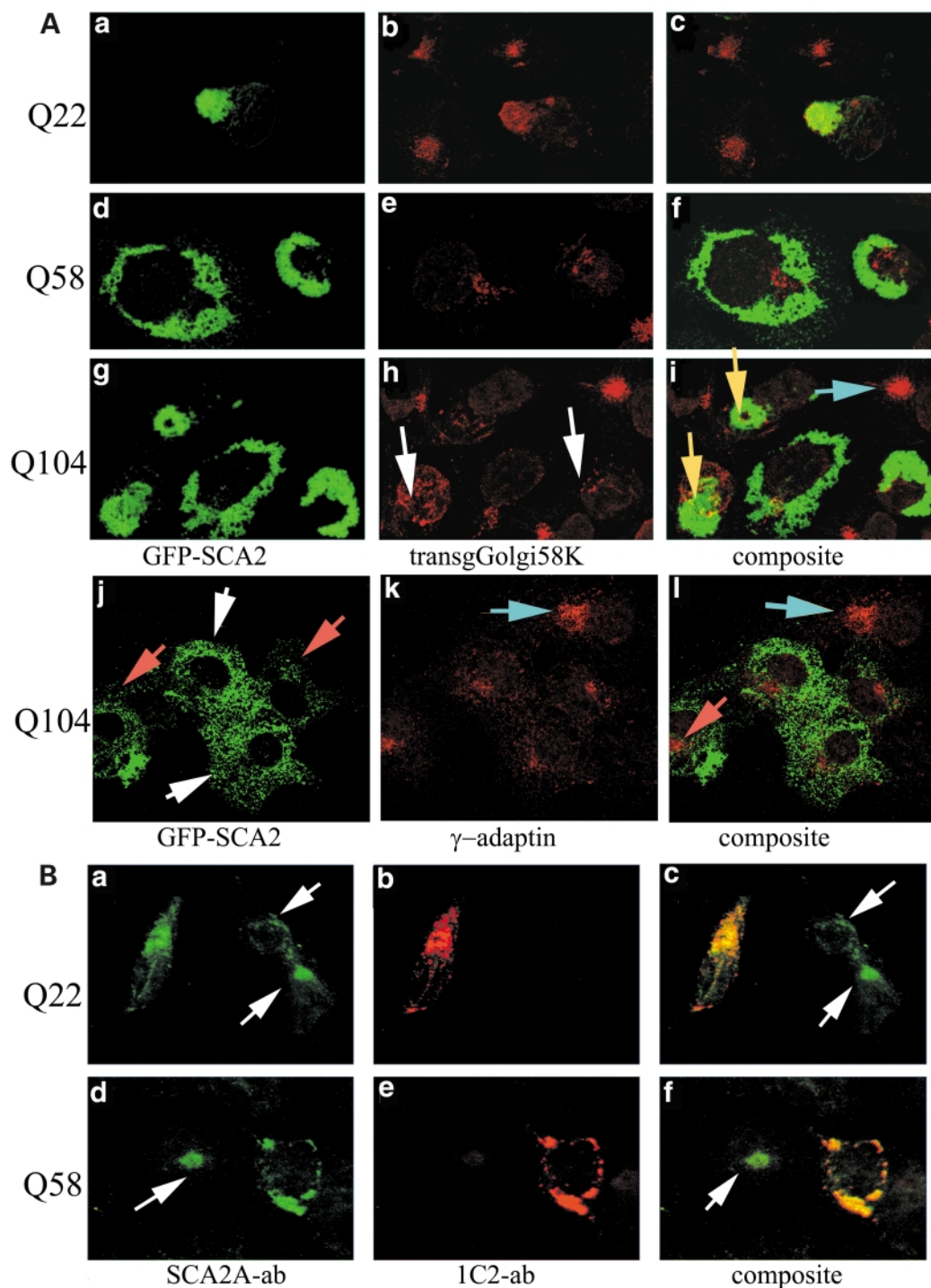


Figure 3. (A) Panels a–i: Colocalization of GFP-tagged ataxin-2[Q22] with the transGolgi58K protein, but disruption of normal Golgi labeling by expression of ataxin-2 with expanded polyQ repeats. COS1 cells were transiently transfected with GFP-ataxin-2[Q22] (panels a–c), GFP-ataxin-2[Q58] (panels d–f), and GFP-ataxin-2[Q104] (panels g–i). Cells were then labeled with a monoclonal antibody to transGolgi58K (panels b, e, h) and viewed by confocal laser microscopy. As expected, GFP-ataxin-2[Q22] co-localized with the transGolgi58K protein, while GFP-ataxin-2[Q58] and Q104 redistributed throughout the cytoplasm or formed perinuclear aggregates. A small proportion of the cells expressing GFP-ataxin-2[Q104] formed intranuclear aggregates with GFP-ataxin-2[Q104] (yellow arrows). Labeling of the Golgi apparatus in cell expressing the ataxin-2 with expanded polyQ repeats was altered (white arrow). Note an untransfected cell with an intact and normal Golgi apparatus in panel i (blue arrow). Panels j–l: localization of  $\gamma$ -adaptin (k) in COS1 cells transfected with GFP-tagged ataxin-2[Q104]. White and red arrows show cells overexpressing different amounts of GFP-ataxin-2[Q104]. The blue arrow shows untransfected cell. (B) Expression of untagged human ataxin-2 with 22 or 58 gln repeats in COS1 cells. Panels a–c, COS1 cells transfected with pcDNA-ataxin-2[Q22]; panels d–f, COS1 cells transfected with pcDNA-ataxin-2[Q58]. Cells were co-labeled with antibodies to ataxin-2, SCA2A (panels a and d) and polyQ repeat, 1C2 (panels b and e). Images were acquired using the 100 $\times$  oil immersion lens of the Leica TCSSP. White arrows point to untransfected cells expressing endogenous ataxin-2, which does not label with the 1C2 antibody.

ataxin-2[Q58]. These observations suggest that the incident of Golgi disruption is due to the toxicity resulting from the expansion of the polyQ repeats in ataxin-2.

Expression of ataxin-1, 3 and 7 with expanded polyQ repeats caused cell stress and increased the levels of heat shock proteins (19–23). To examine whether overexpression of GFP-ataxin-2 increases the synthesis of heatshock proteins, cells transiently expressing GFP-ataxin-2 with 22, 58 or 104 polyQ repeats were immunofluorescently labeled with an antibody to the Hsp70 heatshock protein. The levels of Hsp70 were not upregulated in cells expressing exogenous ataxin-2 above the levels found in untransfected cells (data not included). These observations suggest that the disruptions of the Golgi complex (Fig. 3) and cell death (Fig. 4) caused by ataxin-2 with expanded polyQ repeats are not the result of non-specific cell stress resulting from overexpression.

Expansion of the polyQ repeat in ataxin-2 causes cell death and increases the levels of activated caspase-3

To determine whether expansion of the polyQ repeat in ataxin-2 resulted in increased cell death, cells transfected with GFP-ataxin-2[Q22], GFP-ataxin-2[Q58] or GFP-ataxin-2[Q104] expression plasmids were labeled with 0.4% Trypan blue. The proportion of dead cells was calculated by dividing Trypan-blue labeled cells with the total number of cells. As shown in Figure 4A, polyQ repeat expansion caused cell death in PC12 cells, whereas expression of the normal human allele was not different from vector-transfected cells. When the polyQ repeat was expanded to 58 and 104 glutamines, respectively, the percentage of Trypan blue labeled cells increased to  $28 \pm 1.82$  and  $29.58 \pm 2.22$ , respectively, compared with  $9.28 \pm 1.21\%$  for GFP or ataxin-2[Q22]-expressing cells. Although there was a small increase in the number of dead cells in cells expressing GFP-ataxin-2[Q104], the difference was not statistically significant. The transfection efficiency in these experiments (as determined by the percentage of GFP labeled cells) ranged from 30 to 40%; transfection efficiencies within a given experiment were not significantly different for the constructs used.

In COS1 cells, similar observations were made (Fig. 4B). Both length of the polyQ repeat and duration of expression influenced cell death. The greatest amount of cell death was seen in cells expressing ataxin-2[Q104]. Expression of ataxin-2[Q58] caused cell death at levels between those seen with ataxin-2[Q22] and ataxin-2[Q104]. Longer duration of expression increased cell death (except for GFP controls). Interestingly, even overexpression of the normal human ataxin-2 caused a small increase in cell death at 24 h with a further increase at 48 and 72 h.

It has been observed that expansion of the polyQ repeat in disease-associated proteins causes the activation of the caspase pathway (16,26,27,34). To investigate whether the observed cell death *in vitro* was, at least in parts, due to the activation of the apoptotic pathway, we used the TUNEL method to stain transfected cells at 24, 48 and 72 h (Fig. 4C). The TUNEL method stains fragmented DNA in apoptotic cells. The results were very similar to those seen in Trypan blue exclusion experiments. The number of TUNEL-positive cells increased with increasing length of the polyglutamine tract and increasing duration of expression. Again, expression of the normal ataxin-

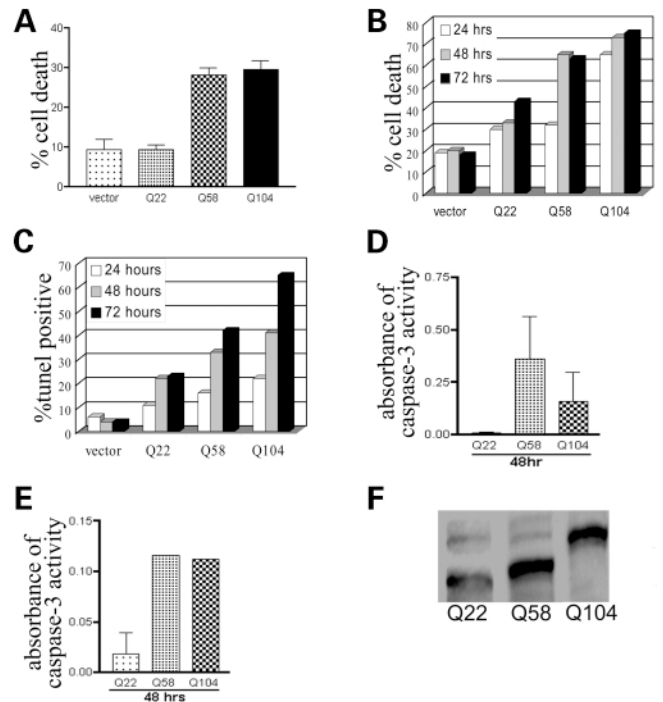


Figure 4. Increased cell death and apoptosis after expression of expanded polyQ repeat ataxin-2. PC12 (A) and COS1 (B–F) cells were transfected with either GFP-tagged ataxin-2 or HA tagged ataxin-2 with 22, 58 or 104 glutamine repeats, respectively. (A) Expression of full-length mutant ataxin-2 in PC12 cells at 48 h increased the number of cells that were unable to exclude Trypan blue (mean  $\pm$  SEM). (B) Mutant ataxin-2 also increases the number of COS1 cells that were unable to exclude Trypan blue (data shown are from one representative experiments with all transfections done simultaneously). (C) Expression of mutant ataxin-2 also resulted in increased numbers of cells with fragmented DNA as demonstrated by TUNEL labeling blue (data shown are from one representative experiments with all transfections done simultaneously). (D,E) Both GFP-tagged (D,  $n = 3$ ) and HA-tagged (E,  $n = 2$ ) mutant ataxin-2 increased the levels of activated caspase-3 compared with wild-type ataxin-2 as demonstrated by the casPACE assay (mean  $\pm$  SEM). (F) Western blot of COS1 cells transfected with constructs expressing GFP-ataxin-2 containing 22, 58 and 104 glutamine repeats and detected with antibody to GFP.

2[Q22] caused an increase in TUNEL-positive cells that was intermediate between GFP control and that seen with ataxin-2[Q58].

To determine whether expression of mutant ataxin-2 increased caspase-3 activity, we used the casPACE assay to measure the levels of caspase-3 activity at 48 h after transfection (Fig. 4D and E). Ataxin-2 with expanded polyQ repeats increased the levels of activated caspase-3 several-fold compared to normal ataxin-2[Q22] ( $P \leq 0.05$ , Fig. 4D). Activation of caspase-3 was seen for ataxin-2 tagged with GFP or with the HA-epitope (Fig. 4E), but the effects of polyQ repeat expansion was more pronounced with the GFP tagged mutant ataxin-2.

The very different levels of apoptosis that we observed were not due to differing transfection efficiencies or protein levels. Western blot analysis of equal amounts of protein extracts from COS1 cells transfected with GFP-ataxin-2[Q22], GFP-ataxin-2[Q58] and GFP-ataxin-2[Q104] showed that the GFP-ataxin-2 plasmid expressed the full-length ataxin-2 with the

expected polyQ repeats at near equal levels (Fig. 4F). Similar to the HA-tagged ataxin-2[Q22] (Fig. 1), the level of GFP-ataxin-2[Q22] was slightly lower compared with the levels of GFP-ataxin-2[Q58] and GFP-ataxin-2[Q104] (Fig. 4F), probably due to increased stability of ataxin-2 with longer polyQ repeats.

## DISCUSSION

### Golgi localization

In this report, we have determined that ataxin-2 is primarily localized to the Golgi apparatus. This observation was supported by co-localization studies of endogenous ataxin-2 and GFP-tagged ataxin-2 (Figs 2 and 3). This localization was also seen with ataxin-2 bearing a HA-tag (not shown). Subcellular fractionation experiments in human cerebral cortex and COS1 cells transiently expressing HA-ataxin-2 (Fig. 1) also indicated that the majority of ataxin-2 co-fractionated with two Golgi markers, the transGolgi58K protein and  $\beta$ -COP. To further confirm that ataxin-2 was a Golgi resident protein, we treated COS1 cells with brefeldin-A. Brefeldin-A reversibly inhibits the transport of proteins from the ER to the Golgi apparatus. Brefeldin-A treatment caused ataxin-2 to redistribute throughout the cytoplasm, as did the transGolgi58K protein (Fig. 2). Finally, deletion of both the ER exit signal and the putative clathrin-recognition motif in ataxin-2 localized it to the cytoplasm (Fig. 2). Together, these data confirm that ataxin-2 is primarily localized in the Golgi complex. These data also support previous observations that ataxin-2 co-localized with its binder, the ataxin-2 binding protein 1 (A2BP1), which was also co-localized with Golgi proteins (32).

In addition to its predominant Golgi localization, ataxin-2 was also found in vesicular bodies and plasma membrane as evidenced by immunofluorescent labeling and subcellular centrifugation (Figs 1 and 2). However, further studies are needed to determine whether vesicular and membrane bound ataxin-2 are the result of the Golgi-resident ataxin-2 co-transported with other Golgi components to the cell membrane, or represent post-translationally modified ataxin-2 being transported to its functional destination. Further investigation is needed to elucidate this phenomenon.

The Golgi localization of ataxin-2 places this protein apart from other members of the polyQ protein family, and suggests that mutant ataxin-2 may induce neuronal cell death by different mechanisms. Expansion of the polyQ repeat displaces the mutant ataxin-2 from the Golgi apparatus, and causes the dispersion of the Golgi apparatus in a majority of COS1 cells that express mutant ataxin-2 (Fig. 3). Furthermore, the number of cells with altered Golgi morphology increased with increasing lengths of the polyQ repeat. The dispersed Golgi structures labeled with Golgi markers but did not contain mutant ataxin-2 (Fig. 3). These observations suggest that mutant ataxin-2 is not efficiently transported into the Golgi apparatus, or that after transport it damages the Golgi to an extent that transGolgi58K protein immunoreactivity is lost.

In previous studies, we found that Purkinje cells in transgenic mice expressing ataxin-2 with 58 glutamine repeats or human SCA2 patients containing ataxin-2 with either 49 or 58

glutamine repeats did not contain intranuclear inclusions (13,31) in contrast to findings with other polyQ proteins (2,35,36). In a study of brains from humans with SCA2, it was found that selected neurons in the brain stem contained intranuclear inclusions (29,30), but no inclusions were found in Purkinje neurons—the predominant neurons that degenerate in SCA2 patients (13,29). In this study, we did not find any evidence that ataxin-2 with 22 or 58 glutamine repeats formed intranuclear inclusions in COS1 cells, although cytoplasmic ataxin-2 aggregates were seen (Fig. 3). However, ataxin-2 with 104 glutamines formed intranuclear inclusions in a small number of transfected cells. Lack of significant amounts of intranuclear ataxin-2 was also confirmed in experiments using differential centrifugation. These findings support the hypothesis that intranuclear inclusions of mutant ataxin-2 are rare and not the primary cause of cell death in SCA2.

Clearance of misfolded proteins is important for the survival of neurons. Degradation of misfolded proteins can occur through either the ubiquitin-dependent proteasomal or the lysosomal pathways. Proteins with an expanded polyQ repeat that were found to be associated with ubiquitin, proteasomal subunits, and heat shock proteins include ataxin-1, ataxin-3, ataxin-7, and huntingtin (htn) (9,10,19,24,37–41). Although we did not find any evidence of ubiquitination of the mutant ataxin-2 in the Purkinje cells of three SCA2 patients and in transgenic mice expressing ataxin-2 [Q58] (13,31), others have found that ubiquitin was co-localized with ataxin-2 in certain neurons in the brain stem that contained intranuclear inclusion in a group of SCA2 patients (29). Ubiquitination, however, was only detected for intranuclear inclusions, not for cytoplasmic aggregates. Furthermore, the levels of a stress response protein, Hsp70, were not increased in cells expressing ataxin-2[Q58] and ataxin-2[Q104]. These observations suggest that mutant ataxin-2 may have a different mechanism of clearance than other ataxin proteins, and mutant ataxin-2 may be less efficiently degraded.

Biochemical analysis of subcellular fractions from cells expressing HA-tagged ataxin-2[Q22] and HA-tagged ataxin-2[Q104] suggests that mutant ataxin-2 did not acquire a different subcellular localization. Both the normal ataxin-2[Q22] and the mutant ataxin-2[Q104] proteins were found in the P3 fractions that were enriched with Golgi and ER components (Fig. 1B). Furthermore, the relative amounts of mutant ataxin-2 were about 3-fold higher than the wild-type ataxin-2. Since both the wild-type and mutant ataxin-2 expression plasmids were identically constructed and the transfected DNA amounts were equal, the detection of larger amounts of HA-ataxin-2[Q104] compared with the wild-type ataxin-2 suggests that the mutant ataxin-2 was inefficiently degraded.

### Golgi dispersion and cell death

The expression of ataxin-2 with an expanded polyQ repeat correlated with both the disruption of the Golgi complex (Fig. 3) and an increase in cell death through apoptosis due to the activation of caspase-3 (Fig. 4). Both of these effects were progressive with increasing lengths of the polyQ repeat. The Golgi complex is composed of a string of stacked cisternal membranes predominantly located in the pericentriolar

area of the cell. During apoptosis, the Golgi complex is fragmented into dispersed clusters of tubulo-vesicular membranes (41) resulting from the cleavage of the Golgi structural protein GRASP65 by caspase-3. Alteration of the Golgi complex by the expression of a polyQ protein with an expanded polyQ repeat was described for huntingtin (42). Overexpression of huntingtin with a polyQ repeat of 46 or 100 glutamines displaced the Golgi complex from its normal pericentriolar position (42). However, the displacement of the Golgi complex occurred only in a few cells overexpressing the mutant huntingtin. Furthermore, mutant huntingtin aggregates colabeled with lysosome markers. This is in contrast to mutant ataxin-2, where Golgi complex dispersion occurred in a majority of cells expressing ataxin-2 with 58 or 104 glutamine repeats. Therefore, Golgi dispersion appears to be a unique aspect of the SCA2 cellular phenotype, probably in part due to the normal Golgi localization of ataxin-2. Future studies will need to elucidate whether Golgi dispersion is the cause or effect of apoptosis. In addition, it will be important to understand whether aggregation of ataxin-2 in the ER and Golgi will impair the proper trafficking of proteins important in function and survival of neurons. It is already evident, however, that cytoplasmic aggregation of mutant ataxin-2 due to polyQ expansion is a powerful inducer of cell death in COS and PC12 cells.

## MATERIALS AND METHODS

### SCA2 plasmid constructions

To generate the GFP-ataxin-2[Q22] and GFP-ataxin-2[Q58] expression plasmids, we removed the full-length SCA2 cDNA insert from the Bluescript-SCA2 cDNA plasmid by cutting it with SpeI and HindIII restriction enzymes to generate an SCA2 cDNA fragment containing nucleotides 149–4481 (5). The SpeI-generated cohesive end was filled using T4 DNA polymerase. The insert was then subcloned unidirectionally in-frame with the pEGFPc2 plasmid vector at the HindIII and SmaI sites.

To generate the GFP-ataxin-2[Q104] expression plasmid, we used a PCR-based method to double the length of the CAG repeat from 58 to 104 CAG repeats. To do this, we created two PCR primer pairs. One pair consisted of primers 149A and 786B. Primer 149A, CTCCAAGCTTCGCCCGCCCTCCGATGCGCT, is an upstream 5' primer and contains the HindIII 5' site (bold letters), while primer 786B, CGGACATTGTGCAGCGCGGGCGGCGGCTGC, contains the BspI site which cuts 16 bases from the recognition site. The 149A–786B PCR fragment was cut with HindIII and BspI to generate a BamHI/BspI 5'-SCA2 fragment containing a CAG repeat with a CG-3' dinucleotide overhang. The second primer pair consists of primers 613A and 1405B. Primer 619A, GCGTGCGAGCCGGTGTATGG, is 49 bases upstream of the Eco57I recognition site, CTGAAG, which cuts 16 bases from its recognition site. Primer 1405B, GGGCACTGTATACGAAGATAAAGTCTATC, is downstream of the BamHI recognition site. The 619A–1405B PCR fragment was cut with BamHI and Eco57I restriction enzymes to generate a BamHI/Eco57I 3'-SCA2 fragment containing a CAG repeat with a CG-5' overhang. Both fragments were ligated with T4 DNA ligase to generate a HindIII–BamHI fragment containing 104 CAG repeats. The HindIII–BamHI fragment was then subcloned into

a GFP-ataxin-2 fragment pre-cut with HindIII and BamHI enzymes to remove the CAG repeat. The final product was purified and sequenced to confirm the number of CAG repeats.

To delete the putative ER/Clathrin recognition domain, we removed the domain by cutting the GFP-ataxin-2 plasmid with XhoI and ClaI. The cDNA fragment was blunt ended and religated in-frame, resulting in an expression plasmid producing a GFP fused to an ataxin-2 lacking a domain containing 43 amino acid residues with the ER exit signal and the putative clathrin-mediated motif. This construct was named GFP-ataxin-2[del43].

### Cell cultures and antibodies

COS1 cells were grown in DMEM medium supplemented with 10% FBS and penicillin/streptomycin, in 37°C incubator with 5% CO<sub>2</sub>. Media were changed every 3 days. One day prior to transfection, 50 000 cells were seeded in a 1 cm coverslip previously coated with 20 µg/ml collagen IV.

For PC12 cells, cells were grown in DMEM containing 10% heat-inactivated serum, 5% fetal bovine serum, and penicillin/streptomycin in a 37°C incubator with 10% CO<sub>2</sub>. Media were changed every 3 days. One day prior to transfection, 60 000 cells were seeded in a 1 cm coverslip previously coated with 40 µg/ml collagen IV or 2 × 10<sup>6</sup> cells per 100 mm<sup>2</sup> tissue culture dish. To induce PC12 neuronal differentiation, PC12 cells were treated with 50 ng/ml of murine 7.5S NGF (Gibco) for 7 days. NGF-containing media were changed every other day.

Mouse monoclonal antibodies to λ-adaptin, transGolgi58K, β-COP proteins, and the FITC- and TRITC-conjugated secondary antibodies were purchased from Sigma. All three λ-adaptin, transGolgi58K and β-COP proteins reside in the periphery of the Golgi apparatus. The antibody against the SCA2A peptide from ataxin-2 was generated in rabbits and characterized as in Huynh et al. (13).

### Transfection methods

Cells were plated 24 h prior to transfection. On the following day, GFP-ataxin-2[Q22], GFP-ataxin-2[Q58] or GFP-ataxin-2[Q104] plasmid was mixed with polyamine transfectant reagent (QIAGEN) and transfected into COS1 cells according to the manufacturer's directions. At the desired time point (24, 48 and 72 h) after transfection, cells were either processed for proliferation and caspase assays or fixed for immunofluorescence labeling. For cells that were examined longer than 24 h after transfection, the medium was changed one additional time. To achieve equal transfection efficiency for all plasmids, we used two methods to quantify the concentration of each plasmid. First, the DNA concentration was measured by spectrophotometer. Then relative amounts of different plasmids were determined by serial dilutions using agarose gel electrophoresis. Based on the results from agarose gel analysis, equal amounts of different expression plasmids were calculated and used for transfection throughout different experiments.

### Chemical treatment

For some experiments, cells were treated with brefeldin A to determine the Golgi localization of ataxin-2. Brefeldin A is a

chemical toxin that reversibly inhibits the transport of proteins from the ER network to the Golgi apparatus, resulting in the disruption in the organization of the Golgi apparatus. For brefeldin A treatment, cells (transfected or nontransfected) were incubated in culture medium containing 10  $\mu$ M of brefeldin A for 30 min. Cells were then washed with cold DPBS and paraformaldehyde fixed for immunofluorescent labeling. To determine whether the effect of the BFA was reversible, BFA treated cells were washed with serum-free medium three times then incubated in normal culture medium. These cells were then again processed for immunofluorescent labeling.

#### Immunofluorescent labeling and confocal laser microscopy

After transfection for 24, 48 or 72 h, cells were fixed with 4% paraformaldehyde in DPBS for 20 min on ice, and incubated in solution A (DPBS, 3% goat serum, 0.05% Triton X-1000) for 30 min. Cells were then incubated with selected mouse or rabbit primary antibody diluted in solution A for 1 h at room temperature. Cells were then washed five times with cold DPBS, and incubated with TRITC conjugated anti-mouse or anti-rabbit IgG diluted in solution A for 1 h at room temperature. Cells were then again washed five times with cold DPBS and covered with a slide in 80% glycerol and 10 mM sodium gallate for fading protection. Images were acquired using a Leica TCSSP (true confocal scanner spectrophotometry) microscope through the oil immersion 100 $\times$  lens. Images were acquired sequentially to prevent bleaching between FITC or GFP with TRITC fluorescence.

#### Protein extraction and western blots

To obtain protein extracts, cells in six-well plates were extracted with 200  $\mu$ l of boiling SDS-PAGE sample buffer at predetermined time points after plasmid transfection. The protein extracts were clarified by 15 min centrifugation using a table-top Beckmann Microfuge. For western blot, 10  $\mu$ l of the protein extract was loaded per well of a 15-well 4–20% gradient, mini SDS-polyacrylamide gel. Proteins were resolved at 100 V for 2 h and transferred to Amersham's nitrocellulose filter overnight at 30 V in the cold room. The filter is then removed from the western blot apparatus, and blocked with 5% non-fat milk for 1 h at room temperature. The blocking solution was then replaced with blocking solution containing either of the following antibodies. Antibodies to GFP (1/1000), polyQ (1C2) (1/1000), and ataxin-2 (SCA2A, 1  $\mu$ g/ml) were used for western blotting. The 1C2 and GFP antibodies were purchased from Chemicon.

#### Subcellular fractionation differential centrifugation methods

Cells or tissues were homogenized in hypotonic lysis buffer (20 mM Hepes, pH 7.2, 1 mM EGTA, protease inhibitor pellet, 0.4% sucrose) at 10<sup>8</sup> cells per 2 ml of lysis buffer. Cells were homogenized by freeze-thaw method. The coarse protein extract was passed through a cheese cloth. The filtered protein extract was then centrifuged at 1000 g for 5 min. The P1 pellet

contained nuclei and plasma membrane. The S1 extract was then centrifuged for 30 min at 10 000 g yielding the P2 pellet enriched with mitochondria, lysosomes and peroxisomes. The S2 fraction was then centrifuged at 100 000 g for 1 h. The supernatant, the S3 fraction, contains mostly solubilized cytosolic protein, while the microsomal pellet, P3, contains proteins in the rough and smooth ER and Golgi. All pellets were washed once with lysis buffer and dissolved in SDS-PAGE buffer at comparable concentration.

#### Cell proliferation and apoptosis assays

For PC12, cells transfected with GFP-ataxin-2[Q22], GFP-ataxin-2[Q58] or GFP-ataxin-2[Q104] were scraped from the tissue culture dishes at 48 h post-transfection. Cells were then stained with 0.4% trypan blue dye to label dead cells and counted using a hemacytometer. The percentage of dead cells was determined by dividing the number of trypan blue-positive cells with the total number of PC12 cells in each well. Each experiment was repeated three times. For COS1 cells, cells transfected for 24, 48 and 72 h were stained with trypan blue dye. The total numbers of GFP-positive or GFP plus trypan blue positive cells were counted in eight different microscope fields of a 20 $\times$  lens objective. For each experiment, a total of 200–300 transfected (GFP positive) cells were counted for each construct. The ratio of cell death was obtained by dividing the number of cells that were positive with both GFP and trypan blue dye by the total number of GFP-positive cells. Each experiment was performed twice.

The activity of activated caspase-3 and the levels of nuclear DNA fragmentation were measured using the CaspACE Colorimetric Assay (Promega) and the DeadEnd Colorimetric TUNEL System (Promega). The CaspACE Assay measures the product of activated caspase-3, and the TUNEL System detects the levels of nuclear DNA fragmentation resulting from cells undergoing apoptosis. To perform these assays, cells were first transfected with GFP-ataxin-2[Q22], GFP-ataxin-2[Q58], or GFP-ataxin-2[Q104] or with HA-ataxin-2 constructs. Forty eight hours after transfection, cells were lysed for the CaspACE Assay. TUNEL labeling was performed according to the manufacturer's protocols. For TUNEL labeling, GFP-positive or GFP plus TUNEL labeled cells were counted at 24, 48 and 72 h post-transfection in eight different microscope fields using a 20 $\times$  lens objective. For each experiment, a total of 200–300 transfected cells were counted. The ratio of TUNEL labeled cells was obtained by dividing the number of cells positive with both GFP and TUNEL dye and the total number of GFP positive cells in each slide.

#### ACKNOWLEDGEMENT

We thank Mr Kolja Wawrowsky (Confocal Laser Spectral Microscope Core Facility at the Burns and Allen Research Institute) for assistance with the confocal laser microscopy. This study was supported by the Carmen and Louis Warschaw endowment, NIH grant RO1-NS33124 to S.M.P. and an NIH long-term disability supplement to D.P.H.

## REFERENCES

- Orr, H.T. (2000) The ins and outs of a polyglutamine neurodegenerative disease: spinocerebellar ataxia type 1 (SCA1). *Neurobiol. Dis.*, 7, 129–134.
- Orr, H.T. and Zoghbi, H.Y. (2001) SCA1 molecular genetics: a history of a 13 year collaboration against glutamines. *Hum. Mol. Genet.*, 10, 2307–2311.
- Nakamura, K., Jeong, S.Y., Uchihara, T., Anno, M., Nagashima, K., Nagashima, T., Ikeda, S., Tsuji, S. and Kanazawa, I. (2001) SCA17, a novel autosomal dominant cerebellar ataxia caused by an expanded polyglutamine in TATA-binding protein. *Hum. Mol. Genet.*, 10, 1441–1448.
- Wanker, E.E. (2000) Protein aggregation and pathogenesis of Huntington's disease: mechanisms and correlations. *Biol. Chem.*, 381, 937–942.
- Pulst, S.M., Nechiporuk, A., Nechiporuk, T., Gispert, S., Chen, X.N., Lopes-Cendes, I., Pearlman, S., Starkman, S., Orozco-Diaz, G., Lunkes, A. et al. (1996) Moderate expansion of a normally biallelic trinucleotide repeat in spinocerebellar ataxia type 2. *Nat. Genet.*, 14, 269–276.
- Riess, O., Laccone, F.A., Gispert, S., Schols, L., Zuhlke, C., Vieira-Saecker, A.M., Herlt, S., Wessel, K., Epplen, J.T., Weber, B.H. et al. (1997) SCA2 trinucleotide expansion in German SCA patients. *Neurogenetics*, 1, 59–64.
- Schols, L., Gispert, S., Vorgerd, M., Menezes Vieira-Saecker, A.M., Blanke, P., Auburger, G., Amoiridis, G., Meves, S., Epplen, J.T., Przuntek, H. et al. (1997) Spinocerebellar ataxia type 2. Genotype and phenotype in German kindreds. *Arch. Neurol.*, 54, 1073–1080.
- Estrada, R., Galarraga, J., Orozco, G., Nodarse, A. and Auburger, G. (1999) Spinocerebellar ataxia 2 (SCA2): morphometric analyses in 11 autopsies. *Acta Neuropathol. (Berl.)*, 97, 306–310.
- Davies, S.W., Turmaine, M., Cozens, B.A., DiFiglia, M., Sharp, A.H., Ross, C.A., Scherzinger, E., Wanker, E.E., Mangiarini, L. and Bates, G.P. (1997) Formation of neuronal intranuclear inclusions underlies the neurological dysfunction in mice transgenic for the HD mutation. *Cell*, 90, 537–548.
- DiFiglia, M., Sapp, E., Chase, K.O., Davies, S.W., Bates, G.P., Vonsattel, J.P. and Aronin, N. (1997) Aggregation of huntingtin in neuronal intranuclear inclusions and dystrophic neurites in brain. *Science*, 277, 1990–1993.
- Lunkes, A. and Mandel, J.L. (1997) Polyglutamines, nuclear inclusions and neurodegeneration. *Nat. Med.*, 3, 1201–1202.
- Paulson, H.L., Perez, M.K., Trotter, Y., Trojanowski, J.Q., Subramony, S.H., Das, S.S., Vig, P., Mandel, J.L., Fischbeck, K.H. and Pittman, R.N. (1997b) Intranuclear inclusions of expanded polyglutamine protein in spinocerebellar ataxia type 3. *Neuron*, 19, 333–344.
- Huynh, D.P., DelBigio, M.R., Ho, D.H. and Pulst, S.M. (1999) Expression of ataxin-2 in brains from normal individuals and patients with Alzheimer's disease and spinocerebellar ataxia type 2. *Ann. Neurol.*, 45, 232–241.
- Garden, G.A., Libby, R.T., Fu, Y.H., Kinoshita, Y., Huang, J., Possin, D.E., Smith, A.C., Martinez, R.A., Fine, G.C., Grote, S.K. et al. (2002) Polyglutamine-expanded ataxin-7 promotes non-cell-autonomous purkinje cell degeneration and displays proteolytic cleavage in ataxic transgenic mice. *J. Neurosci.*, 22, 4897–4905.
- Chai, Y., Shao, J., Miller, V.M., Williams, A. and Paulson, H.L. (2002) Live-cell imaging reveals divergent intracellular dynamics of polyglutamine disease proteins and supports a sequestration model of pathogenesis. *Proc. Natl Acad. Sci. USA*, 99, 9310–9315.
- Saudou, F., Finkbeiner, S., Devys, D. and Greenberg, M.E. (1998) Huntingtin acts in the nucleus to induce apoptosis but death does not correlate with the formation of intranuclear inclusions. *Cell*, 95, 55–66.
- Cummings, C.J., Reinstein, E., Sun, Y., Antalffy, B., Jiang, Y., Ciechanover, A., Orr, H.T., Beaudet, A.L. and Zoghbi, H.Y. (1999) Mutation of the E6-AP ubiquitin ligase reduces nuclear inclusion frequency while accelerating polyglutamine-induced pathology in SCA1 mice. *Neuron*, 24, 879–892.
- Klement, I.A., Skinner, P.J., Kaytor, M.D., Yi, H., Hersch, S.M., Clark, H.B., Zoghbi, H.Y. and Orr, H.T. (1998) Ataxin-1 nuclear localization and aggregation: role in polyglutamine-induced disease in SCA1 transgenic mice. *Cell*, 95, 41–53.
- Cummings, C.J., Mancini, M.A., Antalffy, B., DeFranco, D.B., Orr, H.T. and Zoghbi, H.Y. (1998) Chaperone suppression of aggregation and altered subcellular proteasome localization imply protein misfolding in SCA1. *Nat. Genet.*, 19, 148–154.
- Cummings, C.J., Sun, Y., Opal, P., Antalffy, B., Mestril, R., Orr, H.T., Dillmann, W.H. and Zoghbi, H.Y. (2001) Over-expression of inducible HSP70 chaperone suppresses neuropathology and improves motor function in SCA1 mice. *Hum. Mol. Genet.*, 10, 1511–1518.
- Stenoien, D.L., Cummings, C.J., Adams, H.P., Mancini, M.G., Patel, K., DeMartino, G.N., Marcelli, M., Weigel, N.L. and Mancini, M.A. (1999) Polyglutamine-expanded androgen receptors form aggregates that sequester heat shock proteins, proteasome components and SRC-1, and are suppressed by the HDJ-2 chaperone. *Hum. Mol. Genet.*, 8, 731–741.
- Chai, Y., Koppenhafer, S.L., Bonini, N.M. and Paulson, H.L. (1999) Analysis of the role of heatshock protein (Hsp) molecular chaperones in polyglutamine disease. *J. Neurosci.*, 19, 10338–10347.
- Chai, Y., Koppenhafer, S.L., Shoemith, S.J., Perez, M.K. and Paulson, H.L. (1999) Evidence for proteasome involvement in polyglutamine diseases: localization to nuclear inclusions in SCA3/MJD and suppression of polyglutamine aggregation in vitro. *Hum. Mol. Genet.*, 8, 673–682.
- Lebre, A.S., Jamot, L., Takahashi, J., Spassky, N., LePrince, C., Ravise, N., Zander, C., Fujigasaki, H., Kussel-Andermann, P., Duyckaerts, C. et al. (2001) Ataxin-7 interacts with a Cbl-associated protein that it recruits into neuronal intranuclear inclusions. *Hum. Mol. Genet.*, 10, 1201–1213.
- Nucifora, F.C. Jr, Sasaki, M., Peters, M.F., Huang, H., Cooper, J.K., Yamada, M., Takahashi, H., Tsuji, S., Troncoso, J., Dawson, V.L. et al. (2001) Interference by huntingtin and atrophin-1 with cbp-mediated transcription leading to cellular toxicity. *Science*, 291, 2423–2428.
- Ona, V.O., Li, M., Vonsattel, J.P., Andrews, L.J., Khan, S.Q., Chung, W.M., Frey, A.S., Menon, A.S., Li, X.J., Stieg, P.E. et al. (1999) Inhibition of caspase-1 slows disease progression in a mouse model of Huntington's disease. *Nature*, 399, 263–267.
- Sanchez, I., Xu, C.J., Juo, P., Kakizaka, A., Blenis, J. and Yuan, J. (1999) Caspase-8 is required for cell death induced by expanded polyglutamine repeats. *Neuron*, 22, 623–633.
- Sawa, A., Wiegand, G.W., Cooper, J., Margolis, R.L., Sharp, A.H., Lawler, J.F. Jr, Greenamyre, J.T., Snyder, S.H. and Ross, C.A. (1999) Increased apoptosis of Huntington disease lymphoblasts associated with repeat length-dependent mitochondrial depolarization. *Nat. Med.*, 5, 1194–1198.
- Koyano, S., Uchihara, T., Fujigasaki, H., Nakamura, A., Yagishita, S. and Iwabuchi, K. (1999) Neuronal intranuclear inclusions in spinocerebellar ataxia type 2: triple-labeling immunofluorescent study. *Neurosci. Lett.*, 273, 117–120.
- Pang, J.T., Giunti, P., Chamberlain, S., An, S.F., Vitaliani, R., Scaravilli, T., Martinian, L., Wood, N.W., Scaravilli, F. and Ansorge, O. (2002) Neuronal intranuclear inclusions in SCA2: a genetic, morphological and immunohistochemical study of two cases. *Brain*, 125, 656–663.
- Huynh, D.P., Figueroa, K., Hoang, N. and Pulst, S.M. (2000) Nuclear localization or inclusion body formation of ataxin-2 are not necessary for SCA2 pathogenesis in mouse or human. *Nat. Genet.*, 26, 44–50.
- Shibata, H., Huynh, D.P. and Pulst, S.M. (2000) A novel protein with RNA-binding motifs interacts with ataxin-2. *Hum. Mol. Genet.*, 9, 1303–1313.
- Dinter, A. and Berger, E.G. (1998) Golgi-disturbing agents. *Histochem. Cell Biol.*, 109, 571–590.
- Goldberg, Y.P., Nicholson, D.W., Rasper, D.M., Kalchman, M.A., Koide, H.B., Graham, R.K., Bromm, M., Kazemi-Esfarjani, P., Thornberry, N.A., Vaillancourt, J.P. et al. (1996) Cleavage of huntingtin by apopain, a proapoptotic cysteine protease, is modulated by the polyglutamine tract. *Nat. Genet.*, 13, 442–449.
- Ross, C.A. (1997) Intranuclear neuronal inclusions: a common pathogenic mechanism for glutamine-repeat neurodegenerative diseases? *Neuron*, 19, 1147–1150.
- Chai, Y., Wu, L., Griffin, J.D. and Paulson, H.L. (2001) The role of protein composition in specifying nuclear inclusion formation in polyglutamine disease. *J. Biol. Chem.*, 276, 4489–4497.
- Paulson, H.L., Das, S.S., Crino, P.B., Perez, M.K., Patel, S.C., Gotsdiner, D., Fischbeck, K.H. and Pittman, R.N. (1997) Machado-Joseph disease gene product is a cytoplasmic protein widely expressed in brain. *Ann. Neurol.*, 41, 453–462.
- Perez, M.K., Paulson, H.L., Pendse, S.J., Saionz, S.J., Bonini, N.M., Pittman, R.N. (1998) Recruitment and the role of nuclear localization in polyglutamine-mediated aggregation. *J. Cell Biol.*, 143, 1457–1470.

39. Wyttenbach, A., Carmichael, J., Swartz, J., Furlong, R.A., Narain, Y., Rankin, J. and Rubinsztein, D.C. (2000) Effects of heat shock, heat shock protein 40 (HSP40), and proteasome inhibition on protein aggregation in cellular models of Huntington's disease. *Proc. Natl Acad. Sci. USA*, 97, 2898–2903.
40. Lieberman, A.P., Trojanowski, J.Q., Leonard, D.G., Chen, K.L., Barnett, J.L., Leverenz, J.B., Bird, T.D., Robitaille, Y., Malandrini, A. and Fishbeck, K.H. (1999) Ataxin-1 and ataxin-3 in neuronal intranuclear inclusion disease. *Ann. Neurol.*, 46, 271–273.
41. Lane, J.D., Lucocq, J., Pryde, J., Barr, F.A., Woodman, P.G., Allan, V.J. and Lowe, M. (2002) Caspase-mediated cleavage of the stacking protein GRASP65 is required for Golgi fragmentation during apoptosis. *J. Cell Biol.*, 156, 495–509.
42. Kegel, K.B., Kim, M., Sapp, E., McIntyre-Castano, J.G., Aronin, N. and DiFiglia, M. (2000) Huntingtin expression stimulates endosomal-lysosomal activity, endosome tubulation, and autophagy. *J. Neurosci.*, 20, 7268–7278.